jmb Article

An Unusual Dimeric Small Heat Shock Protein Provides Insight into the Mechanism of This Class of Chaperones

Eman Basha[1,2], Christopher Jones[1], Anne E. Blackwell[1], Guilong Cheng[1], Elizabeth R. Waters[3], Kara A. Samsel[1], Masood Siddique[4], Virginia Pett[5], Vicki Wysocki[1] and Elizabeth Vierling[6]

*1 - **Department of Chemistry and Biochemistry,** University of Arizona, Tucson, AZ 85721, USA*
*2 - **Department of Botany,** Tanta University, Tanta 31527, Egypt*
*3 - **Department of Biology,** San Diego State University, San Diego, CA 92182, USA*
*4 - **Johann Wolfgang Goethe University,** D-60438 Frankfurt am Main, Germany*
*5 - **Department of Chemistry,** The College of Wooster, Wooster, OH 44691, USA*
*6 - **Department of Biochemistry and Molecular Biology,** University of Massachusetts, Amherst, MA 01003, USA*

***Correspondence to Elizabeth Vierling:** Department of Biochemistry and Molecular Biology, University of Massachusetts, 710 North Pleasant Street, Amherst, MA 01003, USA. vierling@biochem.umass.edu*
http://dx.doi.org/10.1016/j.jmb.2013.02.011
Edited by M. F. Summers

Abstract

Small heat shock proteins (sHSPs) are virtually ubiquitous stress proteins that are also found in many normal tissues and accumulate in diseases of protein folding. They generally act as ATP-independent chaperones to bind and stabilize denaturing proteins that can be later reactivated by ATP-dependent Hsp70/DnaK, but the mechanism of substrate capture by sHSPs remains poorly understood. A majority of sHSPs form large oligomers, a property that has been linked to their effective chaperone action. We describe AtHsp18.5 from *Arabidopsis thaliana*, demonstrating that it is dimeric and exhibits robust chaperone activity, which adds support to the model that suboligomeric sHSP forms are a substrate binding species. Notably, like oligomeric sHSPs, when bound to substrate, AtHsp18.5 assembles into large complexes, indicating that reformation of sHSP oligomeric contacts is not required for assembly of sHSP–substrate complexes. Monomers of AtHsp18.5 freely exchange between dimers but fail to coassemble *in vitro* with dodecameric plant cytosolic sHSPs, suggesting that AtHsp18.5 does not interact by coassembly with these other sHSPs *in vivo*. Data from controlled proteolysis and hydrogen–deuterium exchange coupled with mass spectrometry show that the N- and C-termini of AtHsp18.5 are highly accessible and lack stable secondary structure, most likely a requirement for substrate interaction. Chaperone activity of a series of AtHsp18.5 truncation mutants confirms that the N-terminal arm is required for substrate protection and that different substrates interact differently with the N-terminal arm. In total, these data imply that the core α-crystallin domain of the sHSPs is a platform for flexible arms that capture substrates to maintain their solubility.

Introduction

The small heat shock proteins (sHSPs) and related α-crystallins are a virtually ubiquitous protein family, the majority of which have chaperone activity.[1–4] sHSPs have a high capacity for ATP-independent binding of nonnative protein substrates, thereby preventing irreversible substrate aggregation and facilitating subsequent substrate refolding (or possibly degradation) by other ATP-utilizing components of the protein quality control network.[3] In addition to accumulating during heat, oxidative and other stresses, a number of sHSPs are major components of normal cells, and expression and/or mutation of sHSPs are linked to multiple diseases of protein misfolding, including neurodegenerative diseases, myopathies and cataract.[3,5–7] Understanding the mechanism of sHSP action is, therefore, critical to many aspects of cell function in normal and in stressed or diseased states.

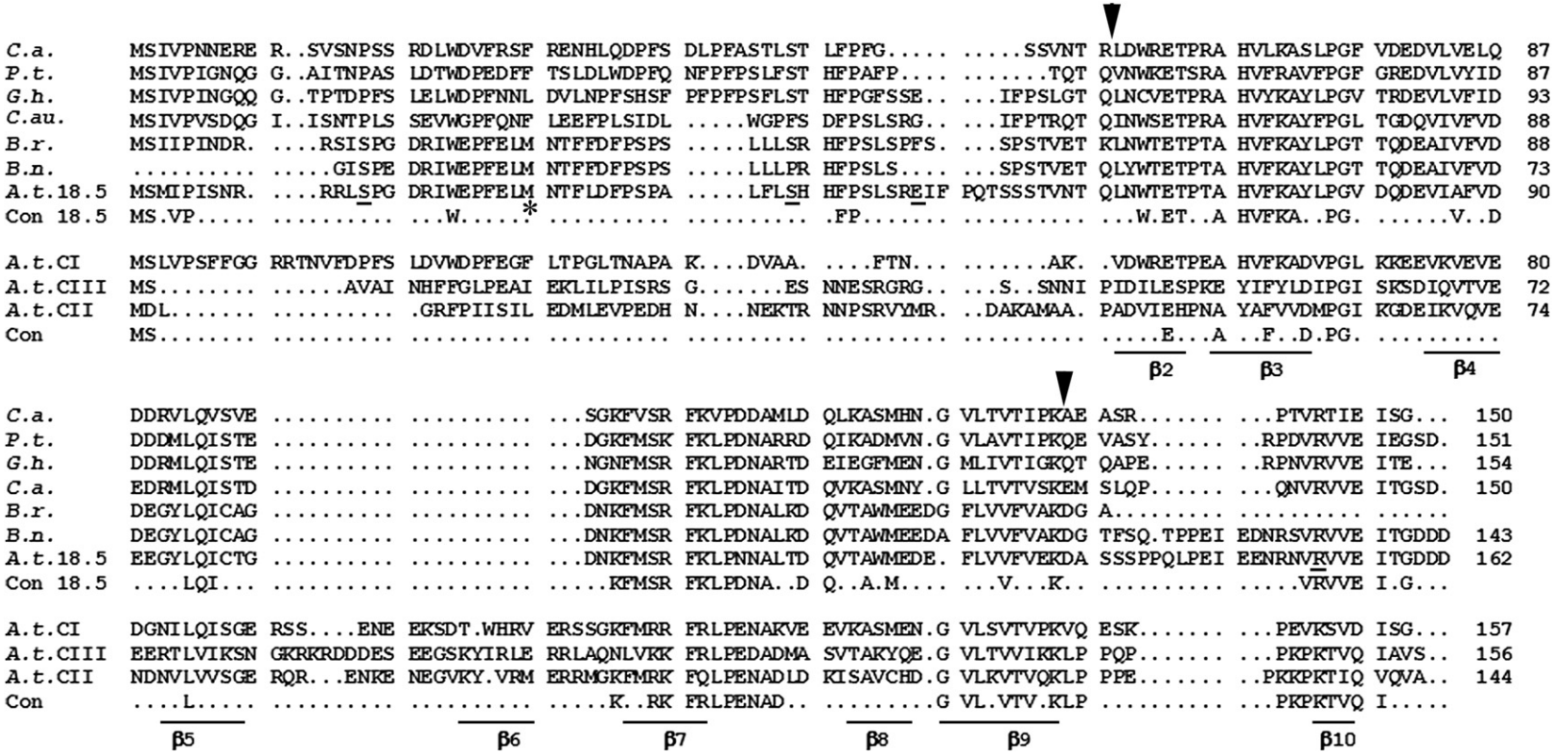

Fig. 1. AtHsp18.5 and homologues are unusual cytosolic plant sHSPs lacking β-strand 6. Alignment of AtHsp18.5 (A.t.18.5) with homologues from *C. avellana* (*C.a.*), *P. trichocarpa* (*P.t.*), *G. hirsutum* (*G.h.*), *C. aurantium* (*C.au.*), *B. rapa* (*B.r.*) and *B. napus* (*B.n.*) compared to other cytosolic sHSPs from classes I, II and III[33] represented by *A. thaliana* Hsp17.4-CI, Hsp17.7-CII and Hsp17.4-CIII. Secondary structural elements are based on alignment with TaHsp16.9.[9] The ACD comprises β2 through β9 (delimited by arrowheads). Consensus sequences for AtHsp18.5 and homologues or for all proteins are shown. Residues corresponding to the beginning and to the end of the truncated proteins as discussed in the text are underlined.

sHSPs are defined by a conserved α-crystallin domain (ACD) of ~90 amino acids flanked by a nonconserved N-terminal arm and a short C-terminal extension.[3,8] A majority of these small proteins (12–42 kDa) assemble into oligomers of ≥12 subunits. Crystal structures of two oligomeric sHSPs, *Methanococcus jannaschii* (a 24-mer) and *Triticum aestivum* (a dodecamer), showed that the ACD is a seven-stranded IgG-like β-sandwich with topology identical with the Hsp90 cochaperone p23.[9,10] Through strand exchange of a loop containing β6, the monomers of these sHSPs form dimers, the basic building block of the oligomers. The ACD fold is conserved in vertebrate sHSPs, but dimers are formed by antiparallel interactions of β7 due to the absence of the β6 loop.[11–13] Oligomers are assembled from dimers via interactions requiring both the N-terminal arm and the C-terminal extension.

The current model for sHSP chaperone action involves a heat-induced structural change (also facilitated by phosphorylation in mammalian sHSPs), which exposes hydrophobic binding sites for denaturing substrate.[14–17] Unlike GroEL and Hsp70, sHSPs can bind up to an equal mass of substrate, and the resulting sHSP–substrate complexes are large and heterogeneous.[14,18–22] Release and refolding of substrate requires Hsp70/DnaK and ATP and can be enhanced by Hsp100/ClpB or GroEL.[23–25] The structural change required for substrate binding is unclear, with data supporting enhanced subunit exchange between the highly dynamic sHSP oligomers,[16] stable oligomer dissociation to suboligomeric species[9,15] or conformational alterations in tertiary structure not involving oligomer disruption.[17,26] Sites of sHSP–substrate interaction are also poorly defined, as these sites appear to include those required for oligomerization, making it difficult to separate these functions. However, increasing evidence indicates that the N-terminal arm is a major mediator of substrate binding.[17,18,27–31]

Genomic data have expanded our knowledge on the sHSP family, with bioinformatics identifying over 8000 sHSP sequences from bacteria, archaea and all phyla of higher organisms.[8,32] We have focused on sHSPs in higher plants, where 12 distinct gene families have been identified.[33] By studying diverse plant sHSPs, we have sought to define fundamental features of the sHSP chaperone mechanism. Here we describe novel structural properties and chaperone activity of AtHsp18.5, a nuclear/cytosolic sHSP from *Arabidopsis thaliana*. Remarkably, this sHSP is a stable dimer, rather than an oligomer, but exhibits robust chaperone activity. Unlike other plant sHSPs, AtHsp18.5 lacks the β6 loop involved in dimerization of other plant and bacterial sHSPs, indicating that it must have a distinct dimer interface. We find properties and activity of AtHsp18.5 to provide new insights into the mechanism of this ubiquitous chaperone family.

Results

AtHsp18.5 is heat induced and behaves as a dimer

Sequences of AtHsp18.5 and homologous proteins from other plant species are aligned in Fig. 1 compared to representative sequences of three other classes of cytosolic sHSPs from plants. These sHSPs share seven predicted β-strands that characterize the ACD and the characteristic C-terminal I/V-x-I/V motif, but notably, compared to other plant, bacterial and yeast sHSPs, AtHsp18.5 and homologues have a deletion of ~20 residues comprising a loop containing β6. In dodecameric wheat Hsp16.9 (a class I plant sHSP), the β6 loop incorporates into a β-sheet of another monomer to form the fundamental dimeric unit of the oligomer.[9,10] Vertebrate sHSPs also lack the β6 loop and dimerize through antiparallel interaction of extended β7 strands.[12,13,34] These sequence and structural data suggest that quaternary assembly of AtHsp18.5 and homologues is potentially different from either the vertebrate or plant sHSPs.

To investigate the quaternary structure of AtHsp18.5, we analyzed purified recombinant AtHsp18.5 compared to the well-characterized dodecameric, cytosolic class I sHSP, PsHsp18.1, from *Pisum sativum*.[14,35] Non-denaturing PAGE (Fig. 2a) reveals that AtHsp18.5 migrates much faster than the 217-kDa PsHsp18.1 dodecamer and at a position consistent with the molecular mass of a dimer. Glutaraldehyde cross-linking (Fig. 2b) produced primarily a doublet indicative of dimeric structure, and no higher-molecular-weight forms were observed, even at a 3000 molar excess of glutaraldehyde (data not shown). We attribute the cross-linked doublet of AtHsp18.5 to varying structures of a dimeric cross-linked species. A minor species above 56 kDa is likely a contaminant, as it does not increase with increasing glutaraldehyde concentrations. This pattern of cross-linking is in stark contrast to the dimeric and higher-molecular-weight species observed for dodecameric PsHsp18.1.

For direct determination of molecular mass, AtHsp18.5 was analyzed by nano-electrospray ionization mass spectrometry (nano-ESIMS) (Fig. 2c) and found to be dimeric. Note that the nano-ESIMS method maintains noncovalent protein structure and has been used to characterize multiple dodecameric plant sHSPs.[36–38] The dimeric structure of AtHsp18.5 was also confirmed in solution by sedimentation velocity analytical ultracentrifugation.

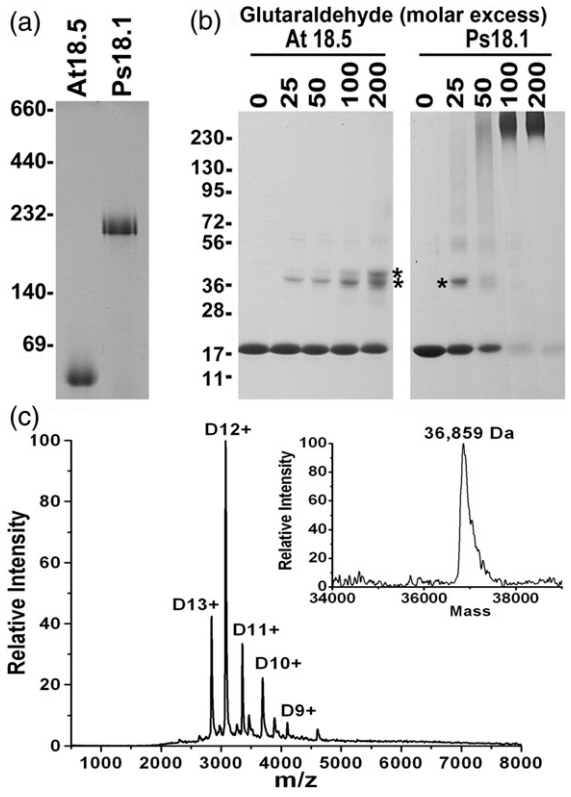

Fig. 2. Native AtHsp18.5 is dimeric. (a) Non-denaturing PAGE of 15 µl of 24 µM sHSP. (b) We cross-linked 24 µM sHSPs with glutaraldehyde at the indicated molar ratios and analyzed 15 µl by SDS-PAGE. Asterisks indicate position of the dimeric cross-linked species. (c) Nano-ESIMS of native AtHsp18.5. Inset shows dimer mass as determined from the deconvoluted spectrum.

Sedimentation of between 2.5 and 30 µM protein at 20 °C yielded a single species with an estimated mass of 81–92% that of a dimer. No higher mass forms were detected and no distinct monomeric form was observed, although the lower mass estimate indicates some degree of dissociation, which is consistent with subsequent monomer exchange measurements (see below). The absence of a discrete monomeric species in the profiles indicates that the K_d is in the low micromolar range.

We further determined that AtHsp18.5 dimeric structure is not dependent on disulfide linkage between subunits, as substitution of the single Cys residue (Cys98) with Ala did not alter the dimeric behavior of the protein in any of the above assays (data not shown). We conclude that AtHsp18.5 is a noncovalent dimeric sHSP under all conditions tested.

Although AtHsp18.5 has an atypical quaternary structure, it is heat induced at the mRNA and protein levels, as are other plant sHSPs. Data from the public database show that AtHsp18.5 mRNA increases dramatically at high temperature, and Western analysis shows that the protein is not detected under control conditions but increases in parallel with mRNA accumulation to ~0.005% of total protein under the conditions tested (Supplemental Fig. 1). Thus, AtHsp18.5 may function with other plant cytosolic sHSPs during stress.

Dimeric AtHsp18.5 is an effective chaperone

As the majority of highly active sHSP chaperones are oligomers, it was of significant interest to investigate chaperone activity of the AtHsp18.5 dimer. In a survey of several plant sHSPs, we obtained initial evidence that AtHsp18.5 could protect firefly luciferase (Luc).[33] To extend this work, we tested the ability of AtHsp18.5 to protect Luc and two additional model substrates (malate dehydrogenase, MDH; citrate synthase, CS) from heat-induced insolubility (Fig. 3a and Supplemental Fig. 2). AtHsp18.5 protected MDH as effectively as PsHsp18.1, with full protection achieved at a molar ratio (sHSP:substrate) of 1:1. Full protection of Luc required AtHsp18.5 at a molar ratio of 12:1 (sHSP:substrate), about twice the amount of PsHsp18.1 required. The dimeric sHSP was also six times less efficient in protecting CS, requiring a sHSP:substrate ratio of 18:1 compared to 3:1 for PsHsp18.1 (Supplemental Fig. 2). In all assays, the sHSPs remained fully soluble (data not shown). These data indicate that sHSP dimers are effective chaperones with specific substrates, and furthermore, the differences in efficiency of protection of different substrates indicate that AtHsp18.5 has unique interactions with each substrate.

Oligomeric sHSPs protect substrates by formation of large sHSP–substrate complexes, which has been assumed to involve reformation within the complex of some of the native sHSP oligomeric contacts.[1] To examine the complexes formed between AtHsp18.5 and substrate, we first performed size-exclusion chromatography (SEC) analysis of the sHSPs with MDH, Luc or CS before heating. The absence of interaction between sHSP and substrate before heating is obvious (left-hand panels in Fig. 3b and Supplemental Fig. 2b); the substrate and sHSP elute independently at their predicted molecular mass. Also, as the amount of sHSP was increased, the sHSP peak increases, while the substrate peak remains the same. Because of the similar mass of the dimeric AtHsp18.5 and substrate, there is an overlap in the sHSP and substrate peaks, and substrate appears as a shoulder in the AtHsp18.5 peak (Supplemental Fig. 3).

To examine interaction of the sHSP and substrate after heating, we then performed SEC analysis on the soluble fractions from the substrate protection assays shown in Fig. 3a, at all concentrations at which the sHSPs fully protected substrate. MDH, Luc and CS heated alone do not enter the column

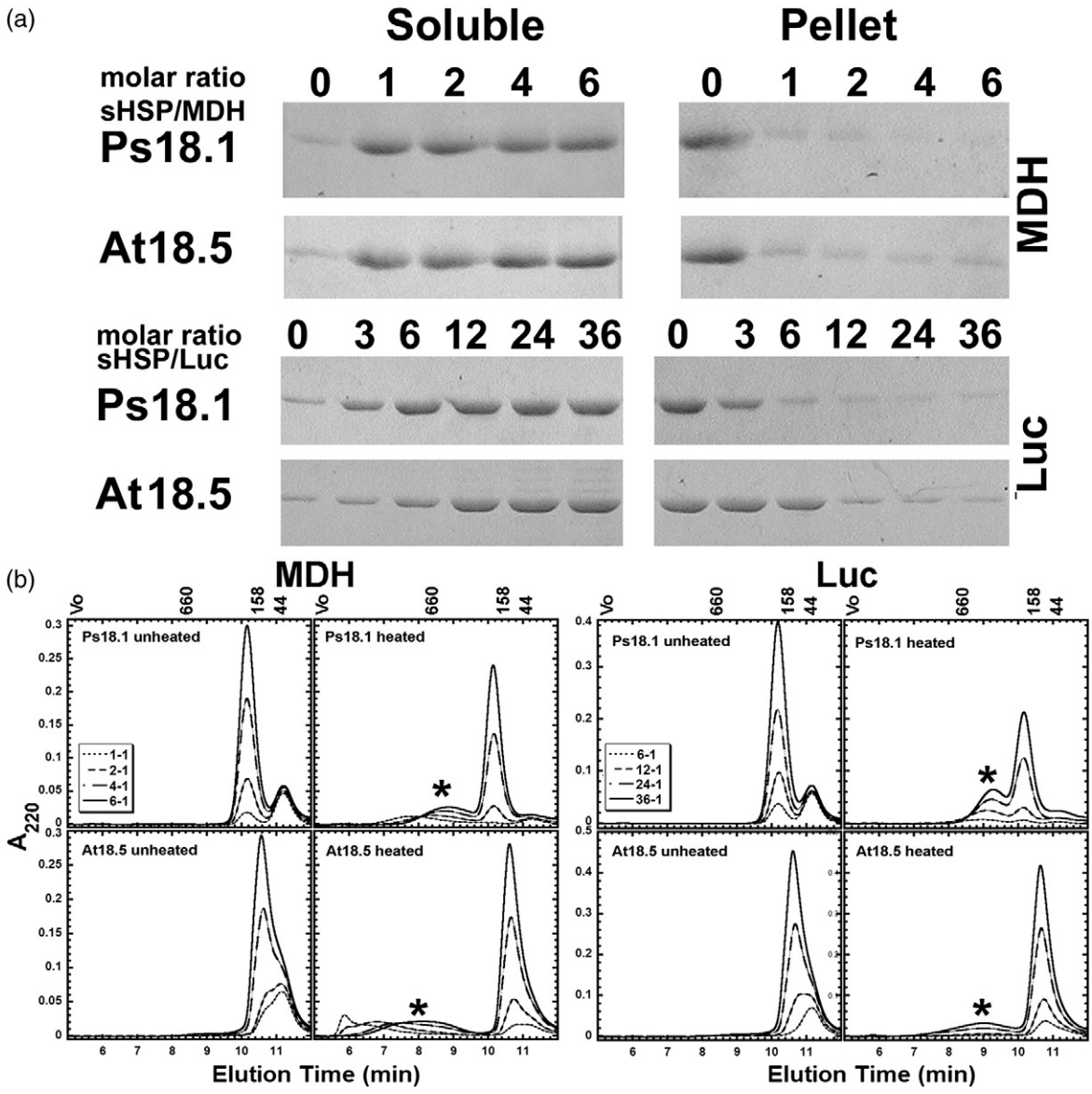

Fig. 3. Dimeric AtHsp18.5 protects substrates from aggregation in large sHSP–substrate complexes. We heated 3 μM MDH or 1 μM Luc with either PsHsp18.1 or AtHsp18.5 at the indicated molar ratios. Heat treatments were 45 °C for 1 h for MDH and 42 °C for 8.5 min for Luc. (a) SDS-PAGE of MDH and Luc from the soluble or pellet fractions after heating at the indicated molar ratio of sHSP to substrate. Gels were stained with Coomassie Blue. (b) SEC analysis of the soluble fractions from (a). Asterisk indicates position of sHSP–substrate complexes.

(Supplemental Fig. 3), and the sHSPs themselves show no change in migration after heating. However, when substrate and sHSP are heated together, new higher-molecular-weight peaks that represent aggregated substrate in complex with sHSP are observed (Fig. 3b, right-hand panels; Supplemental Fig. 3). The native substrate peak disappears completely, and the height of the sHSP peak declines with the appearance of the complex peak. The apparent size of the complexes also decreased with the increase in sHSP:substrate ratio, as seen in previous experiments.[14,18,35] Surprisingly, the AtHsp18.5–substrate complexes span a higher apparent mass range and show more heterogeneity than PsHsp18.1–substrate complexes. This result indicates that although AtHsp18.5 is dimeric, like oligomeric sHSPs, substrate protection involves assembly of complexes containing multiple substrate molecules protected by multiple sHSP subunits.[39] The ability of the AtHsp18.5 dimer to protect substrates demonstrates that oligomeric structure itself or reformation of oligomeric contacts

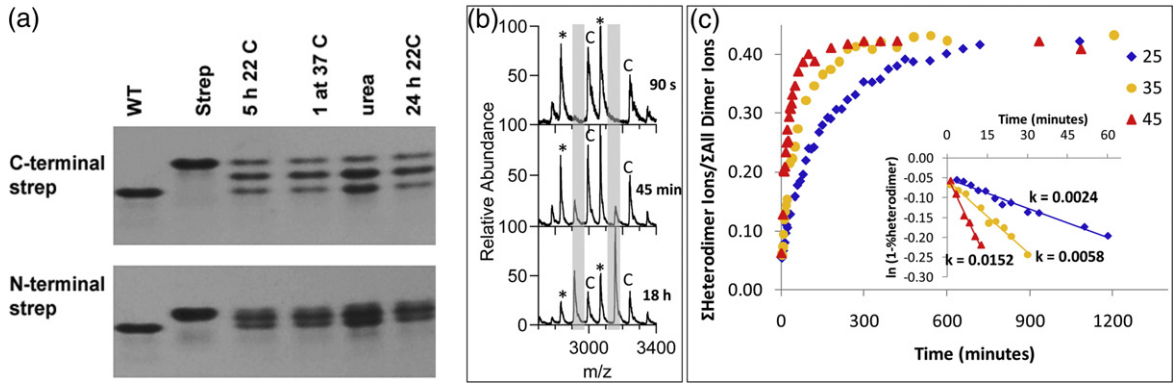

Fig. 4. AtHsp18.5 monomers exchange between dimers at a temperature-dependent rate. (a) Non-denaturing PAGE separation of WT and N- or C-terminally Strep-tagged AtHsp18.5 either alone or after incubation together as indicated. (b) Representative spectra of subunit exchange between WT (*) and AtHsp18.5 carrying a C-terminal Strep tag (C). Spectra from 90 s, 45 min and 18 h show an increase in the relative amount of heterodimer species (gray bars). (c) Rate of appearance of the heterodimer between AtHsp18.5 and C-terminal Strep tag as a function of temperature. Inset: calculated rate constants.

is not required for substrate protection and that sHSP dimers can effectively interact with substrate.

AtHsp18.5 is a dynamic dimer but does not coassemble with other major cytosolic sHSPs

Oligomeric plant sHSPs display quaternary dynamics, typically involving rapid exchange of dimers and slower equilibration of monomers.[37,39] To investigate whether AtHsp18.5 dimers are dynamic, we added an Strep II tag (WSHPQFEK) to either the N-terminus or the C-terminus of AtHsp18.5, mixed either purified tagged protein with wild type (WT) and examined the resulting species on non-denaturing PAGE (Fig. 4a). Note that addition of the tag did not negatively affect AtHsp18.5 chaperone activity (see Fig. 7). In all mixtures, three bands that correspond in migration to a dimer of WT protein, to a dimer of N- or C-Strep-tagged protein or to the heterodimer of WT and Strep-tagged monomers are observed. Therefore, this dimeric sHSP is undergoing monomer exchange. The relative abundance of the three species was the same after different times or temperatures of incubation prior to electrophoresis, and dissociation of the proteins in urea followed by dialysis also resulted in three species (Fig. 4a).

PAGE analysis did not allow an estimate of subunit exchange rate, which might be related to chaperone activity. For rate estimates, we used nano-ESIMS to measure the appearance of heterodimers over time when WT or N- or C-Strep-tagged AtHsp18.5 were incubated together. Figure 4b shows an example of how the mass of the heterodimer comprising WT plus C-terminal Strep-tagged sHSP is easily identified and increases with time of incubation. Rates of exchange were then estimated from nano-ESIMS of incubations performed at 25, 35 or 45 °C (Fig. 4c). Exchange data fit to first-order rate constants that increased ~6-fold from 25 to 45 °C. However, even the rate at 45 °C was 10-fold lower than exchange rates measured for exchange of dimers in dodecameric plant sHSPs.[37,39] These results suggest that the rate of monomer exchange is unlikely to control interaction with substrate.

Because AtHsp18.5 dimers are dynamic, we sought to determine if AtHsp18.5 might function in coassemblies with other sHSPs, as is seen for certain sHSPs in mammals.[6] AtHsp18.5 is found in the plant cytosol[33] and is most closely related to class I cytosolic plant sHSPs (Supplemental Fig. 4a). We therefore examined the ability of AtHsp18.5 to coassemble with each of six class I sHSPs, as well as a more distantly related class II sHSP from *Arabidopsis*. When incubated together at room temperature for 5 h, AtHsp18.5 did not coassemble with any of these sHSPs (Supplemental Fig. 4b). Incubation for up to 24 h at room temperature or heating for 1 h at 35 °C followed by 5 h at room temperature also failed to promote coassembly (data not shown). In contrast, coassembly between different class I sHSPs can be readily observed by this approach.[9,26]

We also investigated whether AtHsp18.5 might be present in large complexes *in vivo* due to assembling with either other sHSPs or unrelated proteins. Non-denaturing electrophoresis followed by Western blotting was performed with purified protein, purified protein added to extracts from control plants or extracts from control or heat-stressed plants. Results revealed AtHsp18.5 migrating only at positions corresponding to dimeric or monomeric species, consistent with the conclusion that the protein does not stably assemble with other cellular components, including dodecameric sHSPs (Supplemental Fig. 5).

Flexibility and core structure of AtHsp18.5

Despite its small size and dimeric structure, we have been unable to obtain diffraction quality crystals of AtHsp18.5. We suspected that this might reflect significant flexibility of the protein. We previously used hydrogen–deuterium exchange (HDX) mass spectrometry (MS) to demonstrate that amide hydrogens in the N-terminal arm and in the C-terminal extension of dodecameric PsHsp18.1 and TaHsp16.9 are in rapid equilibrium with solvent (>70% exchanged in 5 s)[21,40] and, thus, are not involved in highly stable secondary structures. The same technique was applied to AtHsp18.5, and remarkably, the pattern of HDX across AtHsp18.5 was essentially parallel with that of the dodecameric sHSPs (Fig. 5a). The majority

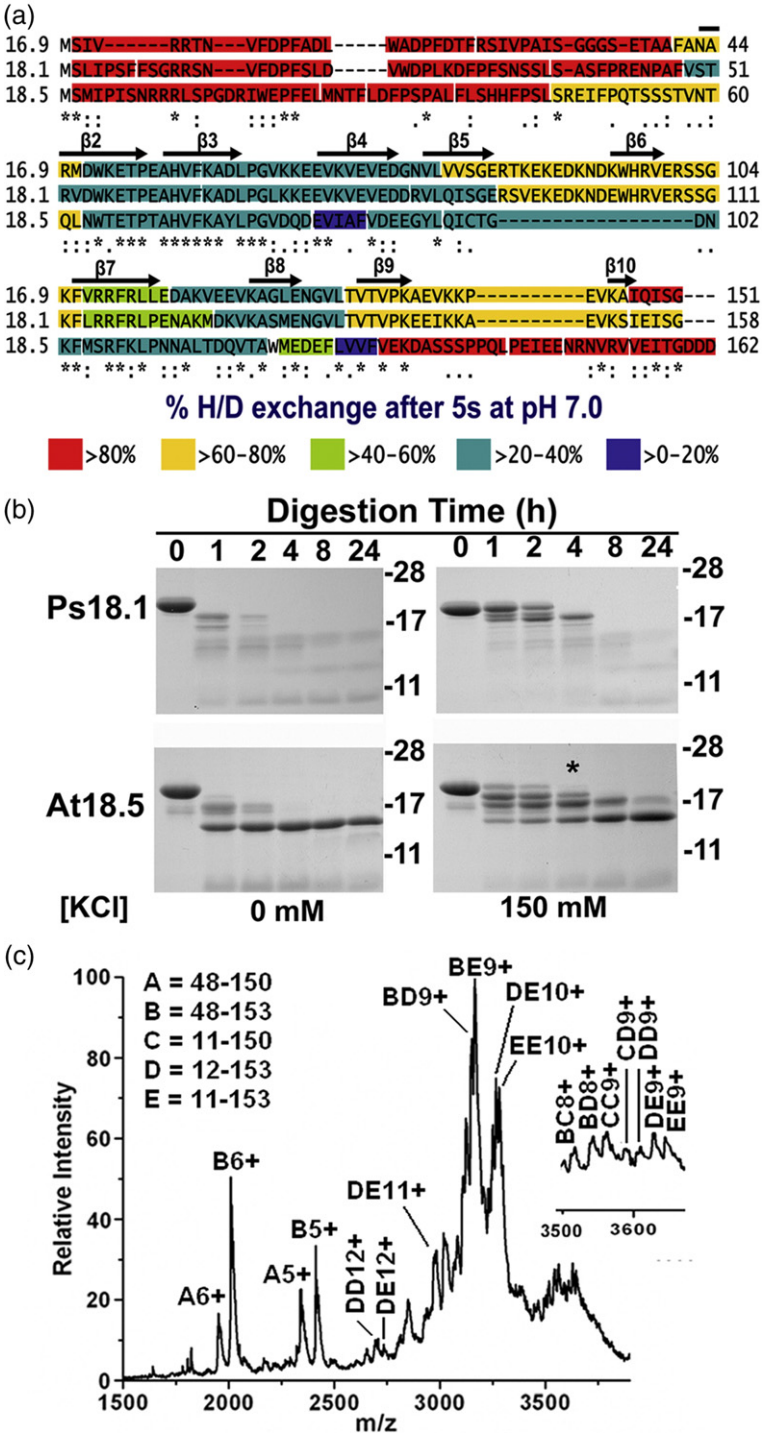

Fig. 5. The AtHsp18.5 ACD forms a stable core flanked by flexible N- and C-termini. (a) Percent HDX for peptides of AtHsp18.5 compared to TaHsp16.9 and PsHsp18.1[21] after a 5-s pulse labeling at pD = 7.5 at room temperature. Each peptide is represented by a colored bar, with the color indicating percentage of amide HDX as shown in the legend. (b) We incubated 24 μM AtHsp18.5 or PsHsp18.1 with trypsin at a 400:1 molar ratio at room temperature for times indicated with or without KCl. Products were analyzed by SDS-PAGE. (c) Nano-ESIMS of the 4-h trypsin digest in 150 mM KCl [asterisk (b)]. Inset shows expansion of the higher *m*/*z* data.

of the protein outside the ACD fully exchanged >80% of amide hydrogens within 5 s, indicating that these regions are not involved in stable secondary structures. In contrast, amide hydrogens in the AtHsp18.5 ACD are highly protected, and this domain is not interrupted by the more readily exchanged β6 loop that is present in PsHsp18.1 and TaHsp16.9.

To study further the AtHsp18.5 structure compared to dodecameric PsHsp18.1, we performed partial proteolysis coupled with MS. AtHsp18.5 and PsHsp18.1 were incubated with trypsin (sHSP/trypsin, w/w, 400/1) in the absence or presence of 150 mM KCl at room temperature for 0–24 h (Fig. 5b). In the absence of KCl, we observed a stable fragment above 11 kDa in the AtHsp18.5 sample after 24 h of trypsin digestion; even doubling the trypsin had no effect on stability of this AtHsp18.5 fragment (data not shown). In contrast, PsHsp18.1 is much more susceptible to trypsin, and after 24 h of digestion in the absence of KCl, only minor amounts of two fragments over 11 kDa remain (Fig. 5b, left panel). Trypsin digestion in the presence of 150 mM KCl significantly slowed the rate of proteolysis. Under these conditions, intermediate digestion products accumulated to higher levels at the earlier time points but the overall pattern of digestion was not otherwise altered, and there was no evidence for a stable fragment corresponding to the ACD in PsHsp18.1.

We used MS to determine the identity of the ~11-kDa, trypsin-resistant fragment from AtHsp18.5. As determined by MS, this fragment corresponds to a combination of residues 48–150 and 48–153 at 11,688 and 12,058 Da, respectively (full-length AtHsp18.5, 162 residues, 18,528 Da) (Supplemental Table 1). These fragments result from cleavage at those trypsin sites closest to, but outside, the ACD. Thermolysin and chymotrypsin digests gave similar results, with no cleavage within the AtHsp18.5 ACD and absence of a similar protected fragment in PsHsp18.1 (data not shown). Proteolysis of TaHsp16.9 yielded results comparable to PsHsp18.1 (data not shown). Therefore, the AtHsp18.5 ACD appears to be folded and assembled in a uniquely protease protected form compared to these dodecameric sHSPs. Considered with the HDX MS data, we conclude that AtHsp18.5 comprises a compact ACD flanked by relatively unstructured “arms”.

Both the N- and C-termini contribute to dimer stability

To obtain insight into the dimer structure, we performed nano-ESIMS on AtHsp18.5 digested with trypsin for 4 h in the presence of KCl (sample with asterisk in Fig. 5b). Figure 5c shows that distinct mass species comprising different protein fragments are resolved. The 48–150/153 fragments are found in multiple monomer peaks (peaks A and B), while the 11–150 and 11/12–153 fragments (C, D and E) are found essentially only in dimer peaks. Interestingly, the 48–153, but not the 48–150, fragment was also found in complex with 11/12–153 and 11–150. These data indicate that part of both the N-terminal arm and the C-terminal extension of at least one subunit contribute to stability of the AtHsp18.5 dimer.

In order to test the importance of different domains in chaperone activity of AtHsp18.5, based on the trypsin cleavage data, we designed and purified several different truncation mutants of AtHsp18.5 comprising residues 13–153, 25–153, 48–153 and 39–162. The 13–153 preparation was found to have ~50% of a fragment comprising residues 25–153 due to use of an alternative start Met (see Fig. 1), and we were not able to obtain pure 13–153. We first estimated the relative dimer stability of the purified proteins using Blue Native PAGE and nano-ESIMS. The full length (WT) and N-Strep and C-Strep constructs migrated at positions consistent with dimeric forms (Fig. 6a), as also seen in Fig. 2 and Supplemental Fig. 5. Based on the relative migration of the truncations, we conclude that the 48–153, 39–162 and 48–150 truncations migrate as monomers. Heating the proteins and separating them at 45 °C did not result in a significant change in the migration of any of the proteins; dimeric forms were stable where present.

Nano-ESIMS provides further information about the relative stability of the dimeric forms of the truncation mutants. The MS conditions used resulted in some dissociation of the native WT dimer, which is typical in experiments investigating noncovalent protein complexes. However, for the full-length proteins, WT, N-Strep and C-Strep, the predominant form observed is the dimer, although somewhat more dissociated species appear in the N-Strep sample. All of the truncation mutants show considerably more monomeric species, consistent with decreased stability of their dimeric forms. Estimating the dimer-to-monomer ratio from the area under the ion peaks at a series of protein concentrations further confirms that the 37–162 and 48–153 truncations form the least stable dimers and that the 25–153 truncation has intermediate stability (Supplemental Fig. 6). While these data do not provide quantitative measures of dimerization constants, they clearly demonstrate that the full-length N-terminal arm and C-terminal extension contribute to dimer stability.

AtHsp18.5 chaperone activity is dependent on the N-terminal arm

We used the truncated AtHsp18.1 mutants to investigate which parts of the protein were required for optimal chaperone activity in protection of MDH and Luc. The ratio of sHSP to MDH that is required to maintain MDH solubility after heating was used as a

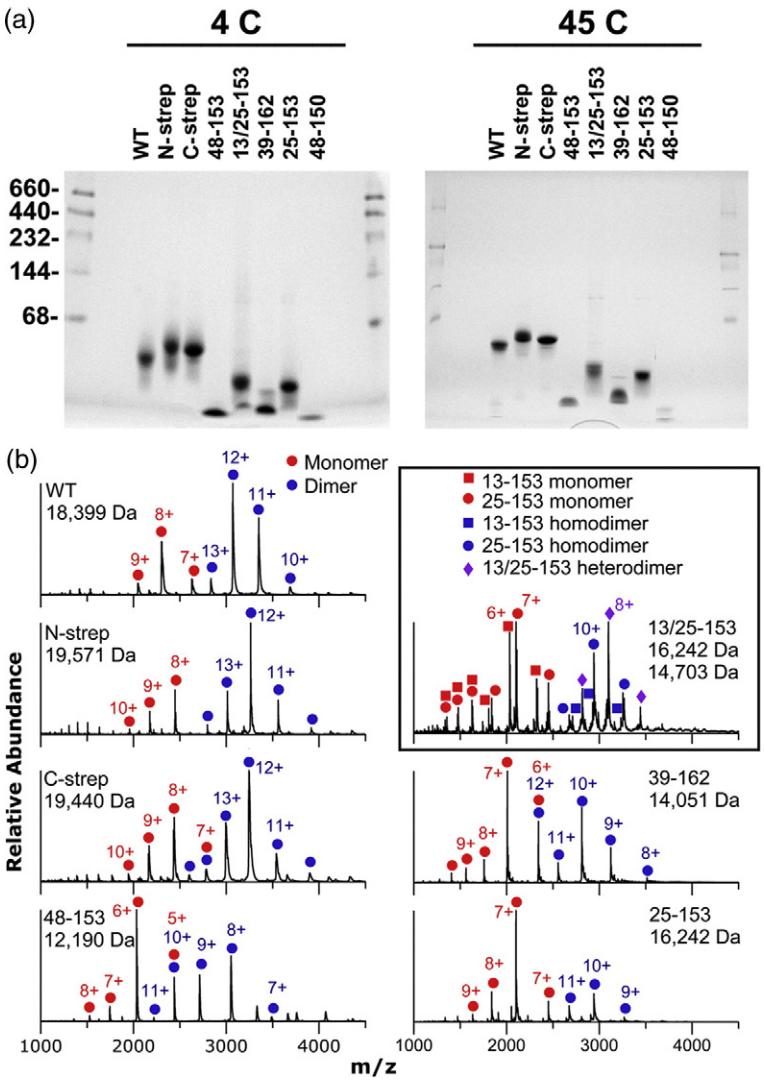

Fig. 6. Detection of dimeric forms of AtHsp18.5 truncated at both the N-terminus or the C-terminus. (a) Blue Native PAGE of the indicated proteins separated at 4 °C (left) or at 45 °C (right). The 48–150 truncation was obtained by trypsin digestion of the WT protein in the absence of KCl as in Fig. 5b. (b) Nano-ESIMS of the indicated proteins at 100 μM, showing detection of different amounts of dimer and monomer.

measure of relative efficiency of the proteins. The N- and C-terminal Strep-tagged proteins actually showed slightly better protection of MDH, and the 13/25–153 preparation showed slightly reduced effectiveness (Fig. 7a). The three proteins missing 25 or more amino acids from the N-terminus (25–153, 48–153 and 39–162) exhibited no chaperone activity in protecting MDH. Using Luc as the heat-sensitive substrate yielded the same results with the exception of the 25–153 truncation and the 13/25–153 preparation (Fig. 7b). While 25–153 had no activity with MDH, it was about half as effective as WT with Luc, and the mixed preparation, 13/25–153, appeared roughly twice as effective as WT. In total, the results show that the ACD alone lacks activity, and the presence of the C-terminus does not compensate for removal of most of the N-terminal arm. Furthermore, the N-terminal arm interacts differently with different substrates and is essential for AtHsp18.5 chaperone activity.

Discussion

The dimeric structure, as well as the ability of the AtHsp18.5 dimer to act as an effective chaperone, is atypical of sHSPs and provides new information relative to how these proteins can achieve substrate protection. The majority of plant, animal and bacterial sHSPs are oligomeric,[3] and only a limited number of other dimeric and even monomeric recombinant sHSPs have been tested for chaperone activity. Both recombinant human HspB6 (Hsp20) and HspB8 (Hsp22) have apparent dimeric structure and can suppress aggregation of some substrates (as shown by light scattering), although dimeric rat HspB6 was reported to exhibit no chaperone activity.[41,42] The apparent dimeric structure of these sHSPs may be limited to the recombinant form, as they assemble into hetero-oligomers with sHSPs and in some cases with other proteins in the mammalian cytosol. Tetrameric and monomeric

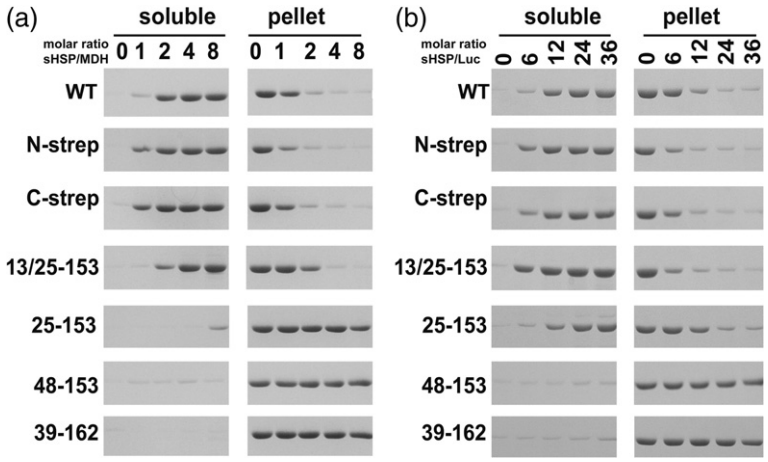

Fig. 7. Truncations of the N- and C-termini alter substrate protection efficiency and the ACD alone is ineffective as a chaperone. We heat denatured 3 μM MDH or 1 μM Luc with the indicated molar ratios of WT or truncated AtHsp18.5 proteins. Denaturation of MDH was for 1 h at 45 °C and 8.5 min at 42 °C for Luc. (a) SDS-PAGE of MDH from the soluble or pellet fractions. (b) SDS-PAGE of Luc from the soluble or pellet fractions. Gels were stained with Coomassie Blue.

sHSPs from *Caenorhabditis elegans* have no detectable chaperone activity.[43–45] The unusual dimer of Tsp36, which has two ACDs per monomer, can prevent aggregation of insulin and CS,[46] but further investigation of its mechanism of action has not been performed. Multiple studies have also tested the activity of sHSP dimers created from native oligomers by N- or C-terminal truncations. Results from these experiments are mixed, with the truncated sHSPs supporting anywhere from good to no protection of specific substrates.[27,47–51] These disparate results with different sHSPs have led to opposing conclusions about the requirement of the oligomeric state for sHSP chaperone activity, as well as the importance of the termini in substrate interactions. The chaperone activity of the AtHsp18.5 dimer clearly demonstrates that substrate binding and formation of sHSP–substrate complexes does not require an oligomeric sHSP to be populated to a significant extent at equilibrium. This result also lends support to the model in which dimers that are released from oligomeric sHSPs, either by subunit exchange[37,39] or temperature-induced dissociation,[9,15,26,50] can act as the substrate binding species. It should be recognized, however, that the availability of dimers may not be the rate-limiting activation step required for sHSP–substrate interaction for all sHSPs.[17,26] Continued study of AtHsp18.5 should provide further insight into sHSP-activating structural changes distinct from changes in oligomeric structure.

The ACD of AtHsp18.5 is unusually stable compared to the ACD of dodecameric plant sHSPs such as PsHsp18.1; the AtHsp18.5 ACD is resistant to proteolysis and shows maximum protection from amide hydrogen exchange throughout the domain (Fig. 5). The AtHsp18.5 ACD is also unique because it lacks the loop containing β-strand 6, which averages ~21 residues in plant sHSPs,[32] and through strand exchange forms the dimer interface. The same region between β5 and β7 is ~14 residues in animal sHSPs[32] and also does not include the β6 loop. The vertebrate proteins dimerize through antiparallel interactions of an extended β7.[11–13,34,47,52] In AtHsp18.5, sequence alignment and structural prediction indicate that only ~4 residues separate β5 and β7, making the AtHsp18.5 ACD similar to the ACD of the structural homologue p23[53] and suggesting that it may have yet a different mode of dimerization than previously characterized sHSPs. Although AtHsp18.5 monomers exchange, the rate of exchange is very slow compared to the time frame of substrate protection, consistent with the dimer, rather than the monomer, being the substrate binding species. Analysis of truncation mutants of AtHsp18.5 indicates that the conserved C-terminal I/V-X-I/V motif (amino acids 155–157), which is involved in oligomerization of other sHSPs,[3] is not required for dimerization. Removal of half or more of the 61-residue N-terminal arm results in destabilization of the dimer. Together with the HDX MS data, the picture emerges of a very stable dimeric ACD core with highly flexible N- and C-terminal arms. Thus, our studies of AtHsp18.5 support the model that the structural flexibility of the N-terminal arms of the dimer allows sHSPs to bind diverse substrates.[3]

The importance of the N-terminal arm in substrate interactions is consistent with activity measurements of AtHsp18.5 truncation mutants. Especially striking is the difference in protection of two substrates, MDH and Luc, by the different truncations. Under the conditions tested, Luc was more effectively protected by truncations that reduced protection of MDH, demonstrating differences in sHSP–substrate contacts for these two proteins. It is also significant that even WT AtHsp18.5 showed very inefficient protection of CS in our assays. Along with previous data, these results demonstrate that there is no single substrate binding site on the sHSPs.[18,31] In addition to removing substrate binding sites, truncations can potentially uncover hydrophobic sites that may otherwise not be primary sites for substrate interaction. This could explain how certain AtHsp18.5

truncations actually enhance protection of Luc (e.g., 13/25–153) and how some substrates can still be protected even by truncated dimeric forms of vertebrate oligomeric sHSPs. Because sHSPs appear to bind exposed hydrophobic surfaces of denaturing proteins, the ability to protect diverse substrates must require varied configurations of available binding surfaces on the sHSP. We propose that the flexible termini of the sHSPs combined with exposed hydrophobic sites on the ACD can provide the necessary variation required to capture different unfolding proteins. The stability of the AtHsp18.5 ACD core may make this protein an excellent model for designing new chaperones with varied N- and C-terminal extensions capable of highly efficient protection of diverse proteins from aggregation.

Materials and Methods

Amino acid alignment

The AtHsp18.5 DNA sequence was used to query the complete TIGR Plant Transcript Assemblies database† with tBlastx, identifying *Corylus avellana* (*C.a.*, AF021807), *Populus trichocarpa* (*P.t.*, Pt826045), *Gossypium hirsutum* (*G.h.*, TA2993.3635), *Citrus aurantium* (*C.au.*, TA1184166), *Brassica rapa* (*B.r.*, TA34073711) and *Brassica napus* (*B.n.*, DC818680) with *e* scores of $1.0 \times e^{-25}$ or lower. The *C. avellana* sequence came from a tBlastx search of the National Center for Biotechnology Information nonredundant database. *P. trichocarpa* (JGI version 1.0‡) and *Oryza sativa* (TIGR) genome sites were also searched. No homologues were detected in *O. sativa*. Cytosolic sHSPs of classes I, II and III are represented by *A. thaliana* Hsp17.4-CI (CAB90950), Hsp17.7-CII (CAB87675) and Hsp17.4-CIII (AAD25777). Sequences were downloaded into BioEdit[54] and aligned using default parameters of ClustalW.[55]

Protein production and quantification

The N- or C-terminal Strep II tag (amino acid sequence: WSHPQFEK) was added to the WT AtHsp18.5 plasmid by polymerase chain reaction. The Hsp18.5 truncation mutants were also generated by polymerase chain reaction introducing a start codon and or a stop codon at the necessary positions. Proteins were purified as previously described[33,35] and quantified using calculated extinction coefficients ($\epsilon_{280} = 16{,}500$ for PsHsp18.1-CI, $\epsilon_{280} = 19{,}615$ for AtHsp18.5-WT and $\epsilon_{280} = 16{,}865$ for 13/25–153 truncation; $\epsilon_{280} = 14{,}115$ for 25–153, 39–162 and 49–153 truncations). Monomeric masses of the purified proteins were confirmed as predicted by MS (Supplemental Table 2).

Gel electrophoresis and cross-linking

Non-denaturing and SDS-PAGE were performed by standard techniques. For analysis of subunit exchange on SDS-PAGE, either proteins were mixed together in 25 mM Tris and 1 mM ethylenediaminetetraacetic acid (pH 7.5) and incubated as previously described or proteins were incubated in 6 M urea at room temperature for 1 h then dialyzed against 5000 volumes of 25 mM Tris and 1 mM ethylenediaminetetraacetic acid (pH 7.5), overnight, prior to electrophoresis.

Blue Native PAGE (5–22% acrylamide) was run at 4 or 45 °C as previously described[56] using 12 µl of 24 µM sHSPs. For cross-linking, sHSPs (24 µM) were incubated with glutaraldehyde at the molar ratios indicated for 1 h at room temperature. The reaction was stopped with a 100-fold molar excess of glycine to glutaraldehyde. Samples were separated by SDS-PAGE (5–15% acrylamide) and stained with Coomassie Blue.

Analytical ultracentrifugation

WT AtHsp18.5 was analyzed be sedimentation velocity centrifugation using a Beckman XL-I dual detection analytical ultracentrifuge with sapphire windows and UV detection at 280 or 230 nm. Five protein concentrations from 2.5 to 30 µM in 10 mM sodium phosphate buffer (pH 7.5) were sedimented at 40,000 rpm, 20 °C, and data were analyzed using SEDFIT and the *c*(*s*) distribution method, with the Lamm equation parameters of partial specific volume of 0.729 ml/g, buffer density of 1.005 g/ml and a confidence interval of 0.68 (1 σ).[57]

MS of subunit exchange

Subunit exchange was observed by native MS. We first buffer exchanged 100 µM solutions of individual proteins into 10 mM (pH 7) ammonium acetate (Sigma-Aldrich, St. Louis, MO) using Micro Bio-Spin columns (Bio-Rad, Hercules, CA) and then placed them in a water bath to equilibrate to the desired temperature. Once equilibrated, equimolar quantities of each protein were mixed and returned to the water bath. Aliquots were periodically removed for mass spectrometric analysis.

Mass spectrometric analysis (nano-ESIMS) was performed on a Q-ToF 2 instrument (Waters Corporation, Milford, MA). We loaded 4–6 µl of protein solution into borosilicate glass capillaries (Corning Incorporated, Corning, NY)[58] pulled in-house with a P-97 micropipette puller (Sutter Instruments, Hercules, CA) and then electrosprayed it using a homebuilt nano-electrospray ionization source. Instrument settings were optimized to maintain intact protein complexes in the gas phase while obtaining clearly resolved peaks.[59] Typical experimental conditions were as follows: capillary voltage, 1.5–2.0 kV; sample cone, 125 V; extractor cone, 1 V; source pressure, $\sim 8.5 \times 10^{-3}$ mbar; analyzer region pressure, 3.1×10^{-5} mbar. For subunit exchange experiments, mass spectra were collected at various intervals between 90 s and 24 h following protein mixing. The amount of heterodimer was quantified relative to the amount of the original homodimeric species to determine the rate of subunit exchange.

MS of intact protein and proteolytic fragments

Typically, 1–5 µl of protein was analyzed essentially as described above with the following specific experimental parameters. MS of intact complexes requires a balance of

conditions for successful ionization and preservation of noncovalent interactions. Optimal ion transmission and preservation of noncovalent interactions was achieved with the following settings: sample cone, 150 V; extractor, 1 V; ion transfer stage pressure, 1×10^{-2} mbar; quadrupole analyzer pressure, 1×10^{-4} mbar; ToF pressure, 3×10^{-6} mbar. For fragment identification, proteolysis fragments were eluted from a STYROS R2 polymer HPLC column (OraChrom, Inc., Woburn, MA) using a gradient of 5–90% acetonitrile (50 μl/min) and injected into a Q-ToF Micro mass spectrometer (Waters, Corporation). Nano-ESIMS on the fragments was as described above for the intact protein.

HDX and MS

Peptide mapping of AtHsp18.5 by HPLC tandem MS was performed as described previously.[21] HDX experiments were initiated by diluting protein ~20-fold into labeling solution (D_2O, 10 mM sodium phosphate, pD = 7.0) to a final concentration of 10 μM. After a 5-s labeling period, protein digestion, peptide identification, mass analysis and back-exchange correction were performed.[21]

Aggregation protection assay

We incubated 1 μM firefly Luc (Promega, San Luis Obispo, CA), 2 μM CS or 3 μM porcine mitochondrial MDH (both from Roche, Germany) with sHSPs at the molar ratios, temperatures and times indicated, and samples were processed as previously described.[18] For analysis of sHSP–substrate complexes, supernatants from aggregation protection assays were applied to a TSKgel G5000PW_{XL} column (flow rate, 1 ml/min) with a mobile phase of 25 mM Na phosphate and 150 mM KCl (pH 7.4).

Acknowledgements

We thank Drs. H. O'Neill and Justin Benesch, N. Jaya and S. Brettschneider for comments on the manuscript. Dr. Chad Park provided expertise for the analytical ultracentrifugation, which was performed in the Analytical Biophysics facility at the University of Arizona. Support for this work is from National Institutes of Health grants GM42762 (E.V.) and GM051387 (V.H.W.), National Science Foundation grant IBN0213128 (E.V.), Pfizer Graduate Research Fellowships in Analytical Chemistry to G.C. and C.J. and a National Science Foundation Graduate Research Fellowship to A.E.B.

Supplementary Data

Supplementary data to this article can be found online at http://dx.doi.org/10.1016/j.jmb.2013.02.011

Received 21 September 2012;
Received in revised form 7 February 2013;
Accepted 8 February 2013
Available online 14 February 2013

Keywords:
chaperone;
α-crystallin domain;
protein flexibility;
subunit exchange;
hydrogen–deuterium exchange

Present addresses: E. Basha, Biology Department, Faculty of Science, Taif University, Taif, Saudi Arabia; C. Jones, Baxter Healthcare Corporation, Round Lake, IL 60073, USA; G. Cheng, Pfizer Global Analytical Research and Development, Groton, CT 06340, USA; V. Wysocki, Department of Chemistry and Biochemistry, The Ohio State University, Columbus, OH 43210, USA.

† http://plantta.tigr.org/index.shtml
‡ http://genome.jgi-psf.org/Poptr1_1/Poptr1_1.home.html

Abbreviations used:
sHSP, small heat shock protein; ACD, α-crystallin domain; CS, citrate synthase; MDH, malate dehydrogenase; MS, mass spectrometry; nano-ESIMS, nano-electrospray ionization mass spectrometry; SEC, size-exclusion chromatography; HDX, hydrogen–deuterium exchange; WT, wild type.

References

1. van Montfort, R., Slingsby, C. & Vierling, E. (2001). Structure and function of the small heat shock protein/alpha-crystallin family of molecular chaperones. *Adv. Protein Chem.* **59**, 105–156.
2. McHaourab, H. S., Godar, J. A. & Stewart, P. L. (2009). Structure and mechanism of protein stability sensors: chaperone activity of small heat shock proteins. *Biochemistry*, **48**, 3828–3837.
3. Basha, E., O'Neill, H. & Vierling, E. (2012). Small heat shock proteins and α-crystallins: dynamic proteins with flexible functions. *Trends Biochem. Sci.* **37**, 106–117.
4. Sudnitsyna, M. V., Mymrikov, E. V., Seit-Nebi, A. S. & Gusev, N. B. (2012). The role of intrinsically disordered regions in the structure and functioning of small heat shock proteins. *Curr. Protein Pept. Sci.* **13**, 76–85.
5. Clark, J. I. & Muchowski, P. J. (2000). Small heat-shock proteins and their potential role in human disease. *Curr. Opin. Struct. Biol.* **10**, 52–59.
6. Vos, M. J., Hageman, J., Carra, S. & Kampinga, H. H. (2008). Structural and functional diversities between members of the human HSPB, HSPH, HSPA, and DNAJ chaperone families. *Biochemistry*, **47**, 7001–7011.
7. Mymrikov, E. V., Seit-Nebi, A. S. & Gusev, N. B. (2011). Large potentials of small heat shock proteins. *Physiol. Rev.* **91**, 1123–1159.

8. Kriehuber, T., Rattei, T., Weinmaier, T., Bepperling, A., Haslbeck, M. & Buchner, J. (2010). Independent evolution of the core domain and its flanking sequences in small heat shock proteins. *FASEB J.* **24**, 3633–3642.
9. van Montfort, R. L., Basha, E., Friedrich, K. L., Slingsby, C. & Vierling, E. (2001). Crystal structure and assembly of a eukaryotic small heat shock protein. *Nat. Struct. Biol.* **8**, 1025–1030.
10. Kim, K. K., Kim, R. & Kim, S. H. (1998). Crystal structure of a small heat-shock protein. *Nature*, **394**, 595–599.
11. Jehle, S., Rajagopal, P., Bardiaux, B., Markovic, S., Kuhne, R., Stout, J. R. *et al.* (2010). Solid-state NMR and SAXS studies provide a structural basis for the activation of αB-crystallin oligomers. *Nat. Struct. Mol. Biol.* **17**, 1037–1042.
12. Bagneris, C., Bateman, O. A., Naylor, C. E., Cronin, N., Boelens, W. C., Keep, N. H. & Slingsby, C. (2009). Crystal structures of α-crystallin domain dimers of αB-crystallin and Hsp20. *J. Mol. Biol.* **392**, 1242–1252.
13. Laganowsky, A. & Eisenberg, D. (2010). Non-3D domain swapped crystal structure of truncated zebrafish αA crystallin. *Protein Sci.* **19**, 1978–1984.
14. Lee, G. J., Roseman, A. M., Saibil, H. R. & Vierling, E. (1997). A small heat shock protein stably binds heat-denatured model substrates and can maintain a substrate in a folding-competent state. *EMBO J.* **16**, 659–671.
15. Haslbeck, M., Walke, S., Stromer, T., Ehrnsperger, M., White, H. E., Chen, S. *et al.* (1999). Hsp26: a temperature-regulated chaperone. *EMBO J.* **18**, 6744–6751.
16. Shashidharamurthy, R., Koteiche, H. A., Dong, J. & McHaourab, H. S. (2005). Mechanism of chaperone function in small heat shock proteins: dissociation of the HSP27 oligomer is required for recognition and binding of destabilized T4 lysozyme. *J. Biol. Chem.* **280**, 5281–5289.
17. Franzmann, T. M., Menhorn, P., Walter, S. & Buchner, J. (2008). Activation of the chaperone Hsp26 is controlled by the rearrangement of its thermosensor domain. *Mol. Cell*, **29**, 207–216.
18. Basha, E., Friedrich, K. L. & Vierling, E. (2006). The N-terminal arm of small heat shock proteins is important for both chaperone activity and substrate specificity. *J. Biol. Chem.* **281**, 39943–39952.
19. Mogk, A., Schlieker, C., Friedrich, K. L., Schonfeld, H. J., Vierling, E. & Bukau, B. (2003). Refolding of substrates bound to small Hsps relies on a disaggregation reaction mediated most efficiently by ClpB/DnaK. *J. Biol. Chem.* **278**, 31033–31042.
20. Friedrich, K. L., Giese, K. C., Buan, N. R. & Vierling, E. (2004). Interactions between small heat shock protein subunits and substrate in small heat shock protein–substrate complexes. *J. Biol. Chem.* **279**, 1080–1089.
21. Cheng, G., Basha, E., Wysocki, V. H. & Vierling, E. (2008). Insights into small heat shock protein and substrate structure during chaperone action derived from hydrogen/deuterium exchange and mass spectrometry. *J. Biol. Chem.* **283**, 26634–26642.
22. Stengel, F., Baldwin, A. J., Bush, M. F., Hilton, G. R., Lioe, H., Basha, E. *et al.* (2012). Dissecting heterogeneous molecular chaperone complexes using a mass spectrum deconvolution approach. *Chem. Biol.* **19**, 599–607.
23. Lee, G. J. & Vierling, E. (2000). A small heat shock protein cooperates with heat shock protein 70 systems to reactivate a heat-denatured protein. *Plant Physiol.* **122**, 189–198.
24. Mogk, A., Deuerling, E., Vorderwulbecke, S., Vierling, E. & Bukau, B. (2003). Small heat shock proteins, ClpB and the DnaK system form a functional triade in reversing protein aggregation. *Mol. Microbiol.* **50**, 585–595.
25. Haslbeck, M., Miess, A., Stromer, T., Walter, S. & Buchner, J. (2005). Disassembling protein aggregates in the yeast cytosol. The cooperation of Hsp26 with Ssa1 and Hsp104. *J. Biol. Chem.* **280**, 23861–23868.
26. Basha, E., Jones, C., Wysocki, V. & Vierling, E. (2010). Mechanistic differences between two conserved classes of small heat shock proteins found in the plant cytosol. *J. Biol. Chem.* **285**, 11489–11497.
27. Kundu, M., Sen, P. C. & Das, K. P. (2007). Structure, stability, and chaperone function of αA-crystallin: role of N-terminal region. *Biopolymers*, **86**, 177–192.
28. Liu, L., Ghosh, J. G., Clark, J. I. & Jiang, S. (2006). Studies of αB crystallin subunit dynamics by surface plasmon resonance. *Anal. Biochem.* **350**, 186–195.
29. Giese, K. C., Basha, E., Catague, B. Y. & Vierling, E. (2005). Evidence for an essential function of the N terminus of a small heat shock protein *in vivo*, independent of *in vitro* chaperone activity. *Proc. Natl Acad. Sci. USA*, **102**, 18896–18901.
30. Haslbeck, M., Ignatiou, A., Saibil, H., Helmich, S., Frenzl, E., Stromer, T. & Buchner, J. (2004). A domain in the N-terminal part of Hsp26 is essential for chaperone function and oligomerization. *J. Mol. Biol.* **343**, 445–455.
31. Jaya, N., Garcia, V. & Vierling, E. (2009). Substrate binding site flexibility of the small heat shock protein molecular chaperones. *Proc. Natl Acad. Sci. USA*, **106**, 15604–15609.
32. Poulain, P., Gelly, J. C. & Flatters, D. (2010). Detection and architecture of small heat shock protein monomers. *PLoS One*, **5**, e9990.
33. Siddique, M., Gernhard, S., von Koskull-Doring, P., Vierling, E. & Scharf, K. D. (2008). The plant sHSP superfamily: five new members in *Arabidopsis thaliana* with unexpected properties. *Cell Stress Chaperones*, **13**, 183–197.
34. Jehle, S., van Rossum, B., Stout, J. R., Noguchi, S. M., Falber, K., Rehbein, K. *et al.* (2009). αB-Crystallin: a hybrid solid-state/solution-state NMR investigation reveals structural aspects of the heterogeneous oligomer. *J. Mol. Biol.* **385**, 1481–1497.
35. Lee, G. J., Pokala, N. & Vierling, E. (1995). Structure and *in vitro* molecular chaperone activity of cytosolic small heat shock proteins from pea. *J. Biol. Chem.* **270**, 10432–10438.
36. Painter, A. J., Jaya, N., Basha, E., Vierling, E., Robinson, C. V. & Benesch, J. L. (2008). Real-time monitoring of protein complexes reveals their quaternary organization and dynamics. *Chem. Biol.* **15**, 246–253.
37. Sobott, F., Benesch, J. L., Vierling, E. & Robinson, C. V. (2002). Subunit exchange of multimeric protein complexes. Real-time monitoring of subunit exchange between small heat shock proteins by using

electrospray mass spectrometry. *J. Biol. Chem.* **277**, 38921–38929.
38. Galhena, A. S., Dagan, S., Jones, C. M., Beardsley, R. L. & Wysocki, V. H. (2008). Surface-induced dissociation of peptides and protein complexes in a quadrupole/time-of-flight mass spectrometer. *Anal. Chem.* **80**, 1425–1436.
39. Stengel, F., Baldwin, A. J., Painter, A. J., Jaya, N., Basha, E., Kay, L. E. *et al.* (2010). Quaternary dynamics and plasticity underlie small heat shock protein chaperone function. *Proc. Natl Acad. Sci. USA*, **107**, 2007–2012.
40. Wintrode, P. L., Friedrich, K. L., Vierling, E., Smith, J. B. & Smith, D. L. (2003). Solution structure and dynamics of a heat shock protein assembly probed by hydrogen exchange and mass spectrometry. *Biochemistry*, **42**, 10667–10673.
41. Bukach, O. V., Seit-Nebi, A. S., Marston, S. B. & Gusev, N. B. (2004). Some properties of human small heat shock protein Hsp20 (HspB6). *Eur. J. Biochem.* **271**, 291–302.
42. van de Klundert, F. A., Smulders, R. H., Gijsen, M. L., Lindner, R. A., Jaenicke, R., Carver, J. A. & de Jong, W. W. (1998). The mammalian small heat-shock protein Hsp20 forms dimers and is a poor chaperone. *Eur. J. Biochem.* **258**, 1014–1021.
43. Leroux, M. R., Ma, B. J., Batelier, G., Melki, R. & Candido, E. P. (1997). Unique structural features of a novel class of small heat shock proteins. *J. Biol. Chem.* **272**, 12847–12853.
44. Kokke, B. P., Leroux, M. R., Candido, E. P., Boelens, W. C. & de Jong, W. W. (1998). *Caenorhabditis elegans* small heat-shock proteins Hsp12.2 and Hsp12.3 form tetramers and have no chaperone-like activity. *FEBS Lett.* **433**, 228–232.
45. Kokke, B. P., Boelens, W. C. & de Jong, W. W. (2001). The lack of chaperonelike activity of *Caenorhabditis elegans* Hsp12.2 cannot be restored by domain swapping with human αB-crystallin. *Cell Stress Chaperones*, **6**, 360–367.
46. Stamler, R., Kappe, G., Boelens, W. & Slingsby, C. (2005). Wrapping the α-crystallin domain fold in a chaperone assembly. *J. Mol. Biol.* **353**, 68–79.
47. Laganowsky, A., Benesch, J. L., Landau, M., Ding, L., Sawaya, M. R., Cascio, D. *et al.* (2010). Crystal structures of truncated αA and αB crystallins reveal structural mechanisms of polydispersity important for eye lens function. *Protein Sci.* **19**, 1031–1043.
48. Feil, I. K., Malfois, M., Hendle, J., van Der Zandt, H. & Svergun, D. I. (2001). A novel quaternary structure of the dimeric α-crystallin domain with chaperone-like activity. *J. Biol. Chem.* **276**, 12024–12029.
49. Fu, X., Zhang, H., Zhang, X., Cao, Y., Jiao, W., Liu, C. *et al.* (2005). A dual role for the N-terminal region of *Mycobacterium tuberculosis* Hsp16.3 in self-oligomerization and binding denaturing substrate proteins. *J. Biol. Chem.* **280**, 6337–6348.
50. Jiao, W., Qian, M., Li, P., Zhao, L. & Chang, Z. (2005). The essential role of the flexible termini in the temperature-responsiveness of the oligomeric state and chaperone-like activity for the polydisperse small heat shock protein IbpB from *Escherichia coli*. *J. Mol. Biol.* **347**, 871–884.
51. Stromer, T., Fischer, E., Richter, K., Haslbeck, M. & Buchner, J. (2004). Analysis of the regulation of the molecular chaperone Hsp26 by temperature-induced dissociation: the N-terminal domail is important for oligomer assembly and the binding of unfolding proteins. *J. Biol. Chem.* **279**, 11222–11228.
52. Clark, A. R., Naylor, C. E., Bagneris, C., Keep, N. H. & Slingsby, C. (2011). Crystal structure of R120G disease mutant of human αB-crystallin domain dimer shows closure of a groove. *J. Mol. Biol.* **408**, 118–134.
53. Weaver, A. J., Sullivan, W. P., Felts, S. J., Owen, B. A. & Toft, D. O. (2000). Crystal structure and activity of human p23, a heat shock protein 90 co-chaperone. *J. Biol. Chem.* **275**, 23045–23052.
54. Hall, T. A. (1999). BioEdit: a user-friendly biological sequence alignment editor and analysis program for WIndows 95/98/NT. *Nucleic Acids Symp. Ser.* **41**, 95–98.
55. Thompson, J. D., Gibson, T. J., Plewniak, F., Jeanmougin, F. & Higgins, D. G. (1997). The CLUSTAL_X windows interface: flexible strategies for multiple sequence alignment aided by quality analysis tools. *Nucleic Acids Res.* **25**, 4876–4882.
56. Swamy, M., Siegers, G. M., Minguet, S., Wollscheid, B. & Schamel, W. W. A. (2006). Blue native polyacrylamide gel electrophoresis (BN-PAGE) for the identification and analysis of multiprotein complexes. *Sci. STKE*, **2006**, pl4.
57. Schuck, P. (2000). Size-distribution analysis of macromolecules by sedimentation velocity ultracentrifugation and lamm equation modeling. *Biophys. J.* **78**, 1606–1619.
58. Jurchen, J. C. & Williams, E. R. (2003). Origin of asymmetric charge partitioning in the dissociation of gas-phase protein homodimers. *J. Am. Chem. Soc.* **125**, 2817–2826.
59. Hernandez, H. & Robinson, C. V. (2007). Determining the stoichiometry and interactions of macromolecular assemblies from mass spectrometry. *Nat. Protoc.* **2**, 715–726.